Mössbauer and Integer-Spin EPR Studies and Spin-Coupling Analysis of the [4Fe-4S]^0 Cluster of the Fe Protein from *Azotobacter vinelandii* Nitrogenase

Sun Jae Yoo,[†] Hayley C. Angove,[‡] Barbara K. Burgess,[‡] Michael P. Hendrich,[†] and Eckard Münck*,[†]

Contribution from the Department of Chemistry, Carnegie Mellon University, Pittsburgh, Pennsylvania 15213, and Department of Molecular Biology and Biochemistry, University of California Irvine, Irvine, California 92697-3900

Received October 26, 1998. Revised Manuscript Received January 4, 1999

Abstract: We have previously shown that the [4Fe-4S] cluster of the Fe protein of nitrogenase from *Azotobacter vinelandii* can be reduced to the all-ferrous state, [4Fe-4S]^0. We have studied here this state with integer-spin EPR and Mössbauer spectroscopy, and analyzed the exchange couplings that give rise to a ground state with cluster spin $S = 4$. The results are as follows: The cluster contains four high-spin ($S_i = 2$) ferrous sites with isomer shift $\delta = 0.68$ mm/s. One site, Fe_A, has $\Delta E_Q = 3.08$ mm/s while the three other sites exhibit ΔE_Q-values between 1.2 and 1.7 mm/s. This asymmetry is surprising in view of the fact that the cluster is suspended at the interface of an α_2 protein dimer. A similar 3:1 symmetry is also evident in the magnetic hyperfine tensors, $\mathbf{A}(i)$, of the four sites; three sites have negative A-values while that of the fourth site, Fe_A, is positive. Analysis of the exchange couplings, assumed to be antiferromagnetic, shows that every possible $S = 4$ ground multiplet that can be constructed from four high-spin ferrous sites must have this property. From Mössbauer spectroscopy we obtained for the $S = 4$ multiplet the zero-field splitting parameter $D = -0.75 \pm 0.05$ cm^{-1}. Moreover, the Mössbauer studies show that the two lowest levels of the spin multiplet are split by $\Delta_{ground} = 0.02$ cm^{-1}. Four pairs of levels from the $S = 4$ multiplet yield integer-spin EPR signals which can be observed, with only minor broadening, at temperatures up to 140 K. Transitions between the two lowest levels yield a sharp resonance at $g = 16.4$. We have simulated the EPR spectra of the all-ferrous cluster in the temperature range from 2 to 120 K and have obtained curves that fit the experimental data with high accuracy. The spin concentration obtained from these simulations is in good agreement with the [4Fe-4S] cluster concentration. Moreover, analysis of the EPR data has revealed that another spin multiplet, most likely an $S = 3$ manifold, becomes populated above 40 K. Exchange coupling (J) among four high-spin ferrous ions yields 85 spin multiplets, 15 of which have $S = 4$. To have an $S = 4$ ground state, two of the six J-values must differ by at least a factor 3, and two others by a factor 2.5. The computed spin projection factors, together with $a_{iso} = -22.4$ MHz of ferrous rubredoxin, yield A_{iso}-values for three of the sites that are in good agreement with the experimental data; Fe_A, however, requires a much smaller a_{iso}-value (-12 to -16 MHz).

Introduction

Nitrogenase, the enzyme system that catalyzes the six-electron reduction of N_2 to ammonia, consists of two separately purified proteins, the Fe protein and the MoFe protein. The Fe protein is a $M_r \approx 60\,000$ dimer of two identical subunits that are bridged by a single [4Fe-4S] cluster coordinated by four cysteine ligands.[1] Each of the two subunits has a binding site for MgATP.[2,3] The MoFe protein is a $M_r \approx 230\,000$ $\alpha_2\beta_2$ tetramer that has two types of metal clusters, the [8Fe−7S] P-clusters and the [Mo−7Fe-9S-homocitrate] FeMoco center.[4−8] Almost everything that is known about the mechanism of this enzyme system comes from in vitro experiments that utilized dithionite as an electron donor.[9] Under those conditions the reactions sequence is as follows. The Fe protein's [4Fe-4S]$^{2+}$ cluster is first reduced by one electron to the +1 oxidation state. The protein then binds two molecules of MgATP, undergoes a critical conformational change, and forms a complex with $^1/_2$ of the MoFe protein.[4,8,10] Within the complex a single electron is transferred from the Fe protein to the MoFe protein P-clusters in a reaction that is somehow coupled to the hydrolysis of both MgATPs.[8,11,12] Subsequently, the two proteins dissociate and

* To whom correspondence should be addressed. Tel.: (412) 268-5058. Fax: (412) 268-1061. E-mail: em40@andrew.cmu.edu.

[†] Carnegie Mellon University.

[‡] University of California Irvine.

(1) Robson, R. L. *FEBS Lett.* **1984**, *173*, 394−398.

(2) Georgiadis, M. M.; Komiya, H.; Chakrabarti, P.; Woo, D.; Kornuc, J. J.; Rees, D. C. *Science* **1992**, *257*, 1653−1659.

(3) Schlessman, J. L.; Woo, D.; Joshua-Tor, L.; Howard, J. B.; Rees, D. C. *J. Mol. Biol.* **1998**, *280*, 669−685.

(4) Howard, J. B.; Rees, D. C. *Chem. Rev.* **1996**, *96*, 2965−2982.

(5) Bolin, J. T.; Campobasso, N.; Muchmore, S. W.; Morgan, T. V.; Mortenson, L. E. In *Molybdenum Enzymes, Cofactors, and Model Systems*; Stiefel, E. I., Coucouvanis, D., Newton, W. E., Eds.; ACS Symposium Series; American Chemical Society: Washington, DC, 1993; pp 186−195.

(6) Kim, J.; Rees, D. C. *Science* **1992**, *257*, 1677−1682.

(7) Peters, J. W.; Stowell, M. H. B.; Soltis, S. M.; Finnegan, M. G.; Johnson, M. K.; Rees, D. C. *Biochemistry* **1997**, *36*, 1181−1187.

(8) Burgess, B. K.; Lowe, D. J. *Chem. Rev.* **1996**, *96*, 2983−3012.

(9) Thorneley, R. N. F.; Lowe, D. J. *Biochem. J.* **1983**, *215*, 393−403.

(10) Thorneley, R. N. F.; Lowe, D. J. *Biochem. J.* **1984**, *224*, 887−894.

(11) Seefeldt, L. C.; Dean, D. R. *Acc. Chem. Res.* **1997**, *30*, 260−266.

(12) Yates, M. G. In *Biological Nitrogen Fixation*; Stacey, G., Burris, R. H., Evans, H. J., Eds.; Chapman and Hall: New York, 1992; pp 685−735.

10.1021/ja9837405 CCC: $18.00
Published on Web 03/04/1999

the process is repeated. As the MoFe protein accumulates electrons one at a time, they are transferred to FeMoco and used to reduce substrates.[8]

This one-electron-at-a-time view of nitrogenase has been challenged recently by the demonstration of the facile reduction of the Fe protein's $[4Fe\text{-}4S]^{1+}$ cluster to the unprecedented $[4Fe\text{-}4S]^{0}$ all-ferrous oxidation state.[13] It has been further established that the all-ferrous Fe protein can bind MgATP, undergo the conformational change, and form a productive complex with the MoFe protein.[14] The all-ferrous Fe protein can then transfer two electrons to the MoFe protein in such a way that they are both used to reduce substrate.[14,15] It has not yet been established if both electrons are transferred from the Fe protein to the MoFe protein prior to complex dissociation. If that is the case, however, it would provide an explanation for the fact that the P-clusters and the FeMo cofactor are both double clusters that might be able to serve as two-electron acceptors. A two-electron-at-a-time mechanism would also be consistent with the observation that all known nitrogenase substrates and intermediates are reduced by multiples of two electrons.[8,11]

The demonstration that the Fe protein's [4Fe-4S] cluster can be reduced to an all-ferrous state has important implications not only for the mechanism of nitrogenase but also for our understanding of [4Fe-4S] cluster chemistry. Prior to this demonstration, clusters of this type had only been known to undergo one-electron redox cycles using either the $[4Fe\text{-}4S]^{3+/2+}$ or the $[4Fe\text{-}4S]^{2+/1+}$ couple,[16] but not both.[17] Currently the $[4Fe\text{-}4S]^{2+/1+/0}$ cluster of the Fe protein is the only example of a cluster that has been stabilized, in the absence of chaotropic reagents, in three core oxidation states. It is also the only protein-bound [4Fe-4S] cluster that has been shown to attain the all-ferrous state, a state that is also unprecedented in model complexes with thiolate ligands. For these reasons we have now performed comprehensive Mössbauer and EPR studies to characterize its electronic and spin structure. Here we report a detailed analysis of the Mössbauer spectra in the framework of an $S = 4$ spin Hamiltonian. We also report parallel mode EPR spectra of the all-ferrous cluster together with spectral simulations that fit the resonances originating from four pairs of sublevels of the $S = 4$ multiplet. Moreover, we provide evidence for the presence of an excited $S = 3$ spin multiplet that becomes thermally populated above 40 K. Finally, we present a detailed analysis of the spin coupling scheme of the four high-spin ferrous ions that gives rise to a ground multiplet with $S = 4$.

Materials and Methods

The Ti(III)citrate-reduced Fe protein sample used in the Mössbauer studies is the same as described previously.[13] Ti(III)citrate-reduced *Azotobacter vinelandii* Fe protein (*Av2*) used for the EPR measurements was prepared by the addition of excess Ti(III)citrate after the removal of sodium dithionite on an anaerobic Sephadex G-25 column, equilibrated with 0.05 M Tris-HCl, pH 8.0, 0.05 M in NaCl. Ti(III)citrate was then diluted to 0.5 mM and the sample concentrated anaerobically in a centricon-30 (Amicon) to an Fe protein concentration of 2.1 mM.

For the deazariboflavin-reduced Fe protein sample, sodium dithionite was removed as described above. An EPR sample containing 0.16 mM Fe protein, 0.2 mM 5′-deazariboflavin and 2 mM EDTA was illuminated outside the glovebox for 2 min using the white light from a slide projector and then frozen in liquid nitrogen.[19]

X-ray Radiolytic Reduction of the $[4Fe\text{-}4S]^{1+}$ Cluster. Sodium dithionite was removed from the Fe protein as described above. A 30% (v/v) glycerol buffered solution was added resulting in a sample containing 0.19 mM Fe protein, 0.05 M Tris-HCl, pH 8.0, 0.02 M in NaCl and 10% v/v glycerol. The EPR sample was irradiated at the Cornell High Energy Synchrotron Source (CHESS). The frozen protein sample was placed in a liquid-nitrogen-filled styrofoam dewar with mylar windows. The sample was irradiated over a 20-mm vertical sweep using a sweep rate of 5 min/mm; the total irradiation time was 100 min.

Spectroscopy. Mössbauer spectra were recorded with two spectrometers operating in the constant acceleration mode. High field spectra (0.15−8 T) were recorded using a Janis Research Super-Varitemp dewar equipped with a superconducting magnet. The 3, 6, and 10 mT magnetic fields were generated by placing two Indox-5 magnets in a Helmholtz configuration around the tail section of a second dewar. Isomer shifts are quoted relative to Fe metal at 298 K. Mössbauer spectral simulations were generated using the WMOSS software package (WEB Research, Edina, MN). EPR spectra were recorded using a Bruker ESP 300 spectrometer equipped with an Oxford ESR 910 liquid helium cryostat, a Au−Fe-chromel thermocouple and an Oxford temperature controller. A Bruker ER 4116 DM dual mode cavity was used to generate the microwave fields, $\mathbf{B}_1$, parallel to the static field, $\mathbf{B}$. The magnetic field was calibrated with an NMR gaussmeter and the microwave frequency was measured with a Hewlett-Packard 5352B counter. Quantitation of the EPR signals in this work has been done relative to a solution of CuEDTA. The concentration of the Cu^{2+} species was determined by plasma emission spectroscopy.

EPR Temperature Calibrations. The Oxford thermocouple temperature was calibrated using a carbon glass resistor temperature probe (CGR-1-1000 Lake Shore Cryotronics). The resistor was placed in a glycerol-filled EPR tube positioned in the sample cavity and connected to the temperature controller. Helium flow was adjusted to optimum conditions, and the CGR and thermocouple temperatures were recorded. EPR spectra of the sample were taken immediately following the temperature calibration using the same helium flow conditions. A second temperature calibration was run after the sample measurement. Comparison of the CGR readings from the two calibrations revealed that the temperature was reproducible within ±1.5 K.

Integer-Spin Simulation Program. Simulations of the EPR spectra are based on diagonalization of the spin Hamiltonian to determine resonance positions, transition probabilities and Boltzmann factors for arbitrary orientations of the magnetic field with respect to the *D*-tensor. For each spin doublet having significant intensity, the contribution to the spectrum at a particular field is summed. The simulated spectra are normalized for angular grid size and field width, and they incorporate the appropriate frequency to field conversion required by normalization of Fermi's Golden Rule for field-swept spectra.[20,21] Thus, the simulated spectra can be quantitatively compared to simulations of a spin standard which can be a simple $S = {}^1/_2$ complex.

Results

Mössbauer Studies. Figure 1 shows zero-field Mössbauer spectra of Ti(III)citrate-reduced *Av2*. The 130 K spectrum exhibits two major doublets. The minority species, doublet 1, has quadrupole splitting, $\Delta E_Q = 2.91$ mm/s, and isomer shift, $\delta = 0.65$ mm/s; at 4.2 K we observed $\Delta E_Q = 3.08$ mm/s and $\delta = 0.68$ mm/s.[22] These parameters are similar to those observed

(13) Angove, H. C.; Yoo, S. J.; Burgess, B. K.; Münck, E. *J. Am. Chem. Soc.* **1997**, *119*, 8730−8731.
(14) Angove, H. C.; Yoo, S. J.; Münck, E.; Burgess, B. K. *J. Biol. Chem.* **1998**, *273*, 26330−26337.
(15) Watt, G. D.; Reddy, K. R. N. *J. Inorg. Biochem.* **1994**, *53*, 281−294.
(16) Holm, R. H.; Kennepohl, P.; Solomon, E. I. *Chem. Rev.* **1996**, *96*, 2239−2314.
(17) In aqueous solution, the [4Fe−4S] cluster of the high-potential iron protein from *Chromatium vinosum* attains the 3+ and 2+ oxidation states. In the presence of 80% dimethyl sulfoxide, however, the cluster can be reduced with dithionite into the 1+ state.[18]
(18) Cammack, R. *Biochem. Biophys. Res. Commun.* **1973**, *54*, 548−554.
(19) Tollen, G.; Hurley, J. K.; Hazzard, J. T.; Meyer, T. E. *Biophys. Chem.* **1983**, *48*, 259−279.
(20) Hendrich, M. P.; Debrunner, P. G. *Biophys. J.* **1989**, *56*, 489−506.
(21) Pilbrow, J. R. In *Transition Ion Electron Paramagnetic Resonance*; Clarendon Press: New York, 1990; Chapter 1.

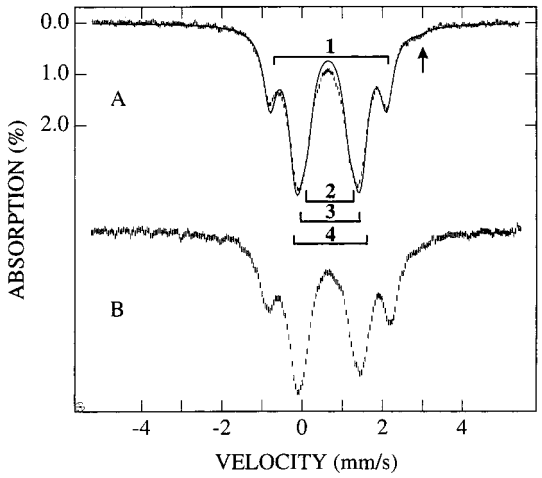

Figure 1. Zero-field Mössbauer spectra of Ti(III)citrate-reduced *Av2* recorded at 130 K (A) and 4.2 K (B). Spectra shown were obtained with the same sample as used for Figures 3, 5, 6, and 7. Protein concentration was 0.92 mM. The solid line in (A) is a superposition of four quadrupole doublets of equal intensity generated with the parameters of Table 1. The four doublets are market by the brackets. A minor ferrous impurity (2% of total Fe) is indicated by the arrow.

Table 1. Quadrupole Splittings and Isomer Shifts of $[4Fe-4S]^0$ *Av2*[a]

	ΔE_Q (mm/s)				
temperature (K)	site 1	site 2	site 3	site 4	δ (mm/s)
4.2	3.08	1.72	1.48	1.24	0.68
130	2.91	1.70	1.45	1.05	0.65
200	2.75	1.68	1.30	0.96	0.62

[a] Isomer shifts, δ, are quoted relative to Fe metal at 298 K. Linewidths were 0.45 mm/s for all components, independent of temperature.

for reduced rubredoxin[23] and thus show that the site represents a high-spin ferrous iron with tetrahedral sulfur coordination. The broader lines of the majority doublet suggest that it contains the contribution of three similar yet distinct sites. We have drawn over the experimental data a theoretical curve generated by assuming four doublets. Although a unique decomposition of the experimental spectrum is not possible, the average isomer shift of sites 2, 3, and 4 is 0.65 mm/s at 130 K and 0.68 mm/s at 4.2 K (see also Table 1). This value of δ, again, is strongly indicative of high-spin Fe^{2+} sites with tetrahedral sulfur coordination. Comparison of the average isomer shift of the four sites (bold arrow in Scheme 1) to those reported for [4Fe-4S] clusters with established core oxidation states reveals that the cluster of Ti(III)citrate-reduced *Av2* is in the $[4Fe-4S]^0$ state. Since site 1 is the unique site of the all-ferrous cluster, we will refer to it with the special designation Fe_A.

To aid the reader, we present in Figure 2 the energy level scheme of an $S = 4$ multiplet. The electronic splitting of this multiplet can be described by the Hamiltonian

$$H_e = D[\mathbf{S}_z^2 - {}^1/_3(S(S+1))] + E[\mathbf{S}_x^2 - \mathbf{S}_y^2] + \beta\mathbf{B}\cdot\mathbf{g}\cdot\mathbf{S} \quad (1)$$

where D and E describe the zero-field splittings and **g** is the g-tensor. We have previously shown[13] that the parameter E/D is near the rhombic limit ($E/D \approx {}^1/_3$) for the all-ferrous cluster.

(22) At 4.2 K, the zero-field spectrum exhibits slightly broader absorption lines than at 40 K. We believe that this broadening is caused by mixing of the electronic φ_1 and φ_2 levels by magnetic hyperfine interactions. For a discussion of this point see ref 54.

(23) Schulz, C.; Debrunner, P. G. *J. Phys. C6* **1976**, *37*, 153−158.

Scheme 1. Average Isomer Shifts, $\delta = (\delta_1 + \delta_2 + \delta_3 + \delta_4)/4$ for Cubane [4Fe−4S] Clusters[a]

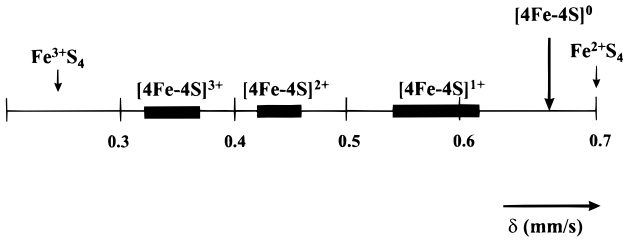

[a] The horizontal bars indicate the range of average δ-values reported for a variety of proteins.

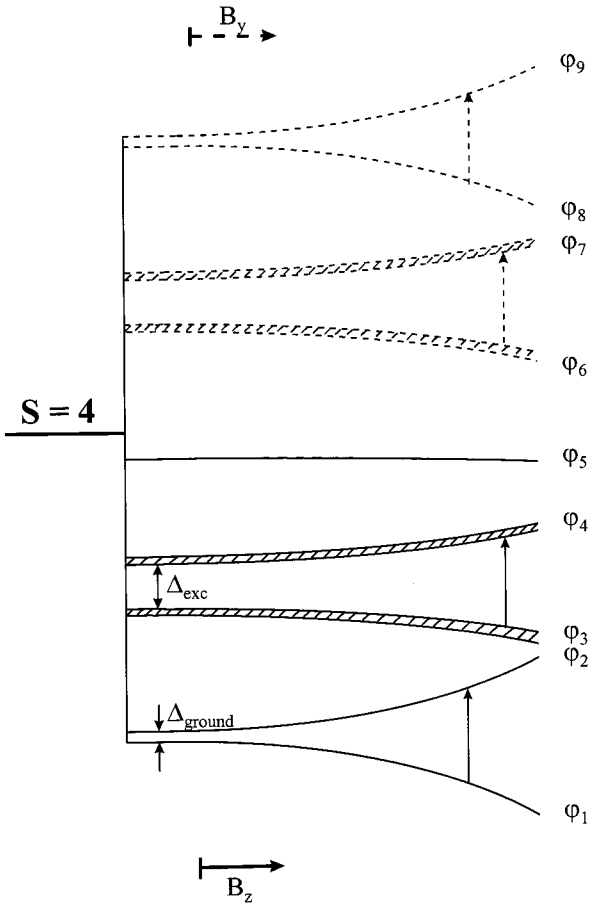

Figure 2. Energy level scheme (not drawn to scale) of the $S = 4$ multiplet. EPR transitions discussed in the text are indicated. Zeeman splitting for the φ_1,φ_2 and φ_3,φ_4 doublets (solid lines) are shown for the case that the applied field **B** is along z, whereas the magnetic splittings (dashed lines) for the upper doublets are indicated for $B = B_y$. Distribution in energies (see text) is illustrated by the shaded areas.

Figure 3 and Figures 5−7 show Mössbauer spectra of Ti(III) citrate-reduced *Av2* recorded in applied magnetic fields up to 8.0 T. As mentioned above, the zero-field spectra of the all-ferrous cluster consist of quadrupole doublets (down to 1.5 K). Figure 3D shows that an applied field as weak as 3 mT induces already sizable magnetic hyperfine fields. This behavior is characteristic of an electronic system with integer-spin for which the splitting between the two lowest sublevels, Δ_{ground}, is very small (for a discussion see ref 24); a fit to the data (see below) suggests that $\Delta_{ground} \approx 0.02\ cm^{-1}$. The spin Hamiltonian of eq 1 predicts, for $B = 0$, that Δ_{exc} (see Figure 2) is substantially larger than Δ_{ground} ($\Delta_{exc} \approx 22\ \Delta_{ground}$). We have used this

(24) Münck, E.; Surerus, K. K.; Hendrich, M. P. *Methods Enzymol.* **1993**, *227*, 463−479.

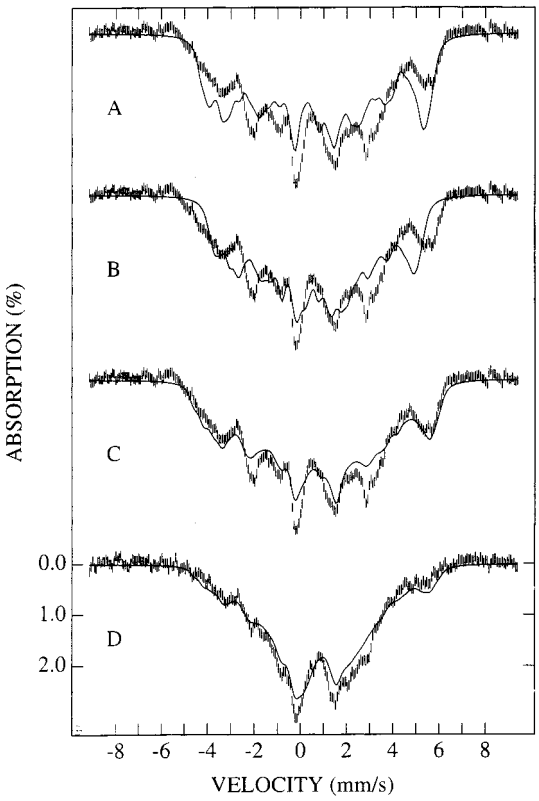

Figure 3. 1.5 K Mössbauer spectra recorded in parallel applied fields of 6 mT (A−C) and 3 mT (D). Solid lines in (A) and (B) are simulations that assume $\Delta_{ground} = 0.015$ and 0.03 cm^{-1}, respectively. Solid lines in (C) and (D) are simulations produced with the parameters listed in Table 2 and with the assumption that Δ_{ground} is distributed about a mean value of 0.02 cm^{-1}.

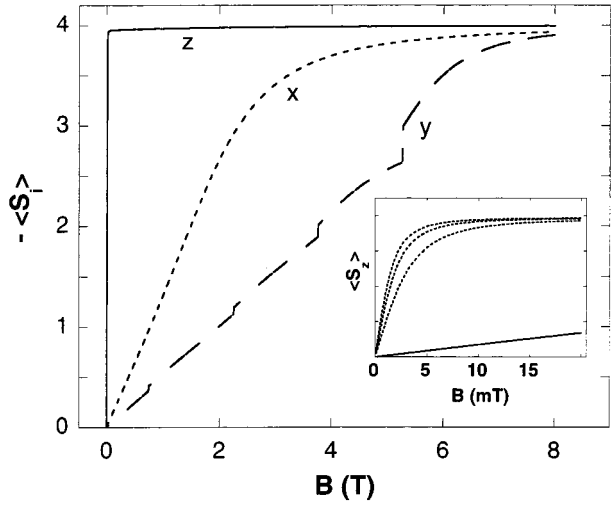

Figure 4. Expectation values, $\langle S_i \rangle$, of the lowest level of the $S = 4$ multiplet, φ_1, assuming that the applied field is along *x*, *y*, or *z*. Inset shows $\langle S_z \rangle$ for the ground doublet (dashed lines) for $\Delta_{ground} = 0.015$ cm^{-1} (top), 0.02 cm^{-1} (middle) and 0.03 cm^{-1} (bottom), as well as $\langle S_z \rangle$ for the φ_3 level (solid line) for $\Delta_{exc} = 0.44$ cm^{-1}. For the given ZFS parameters, level crossings occur along the *y*-direction with increasing applied magnetic field. Because the expectation values of the *lowest* level are plotted, level crossings cause discontinuities in $\langle S_y \rangle$.

circumstance to determine the zero-field splitting parameter *D* by Mössbauer spectroscopy using the following strategy.

The inset of Figure 4 shows the magnitudes of the expectation values of the electronic spin, $|\langle S_z \rangle|$, for the φ_1 and the φ_3 levels.[25] Because $\Delta_{ground} \ll \Delta_{exc}$, $|\langle S_z \rangle|$ saturates much faster for φ_1.

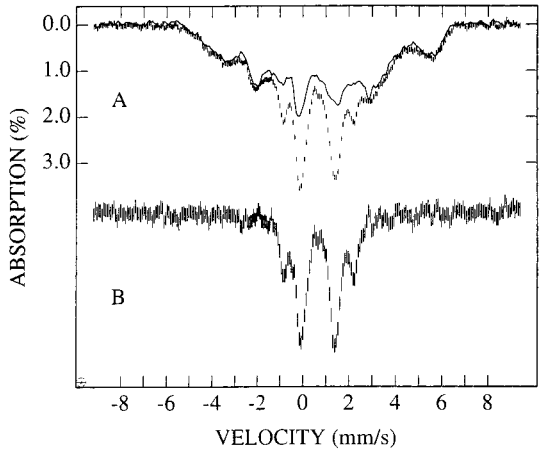

Figure 5. 10 mT Mössbauer spectra of the all-ferrous cluster recorded at 4.2 K (A, bars) and 1.5 K (A, solid line). The spectrum shown in (B) was obtained by subtracting the 1.5 K spectrum of A from that recorded at 4.2 K, after amplitudes of the two spectra were matched at velocities $|v| > 3$ mm/s. The difference spectrum of (B) results from the φ_3,φ_4 levels.

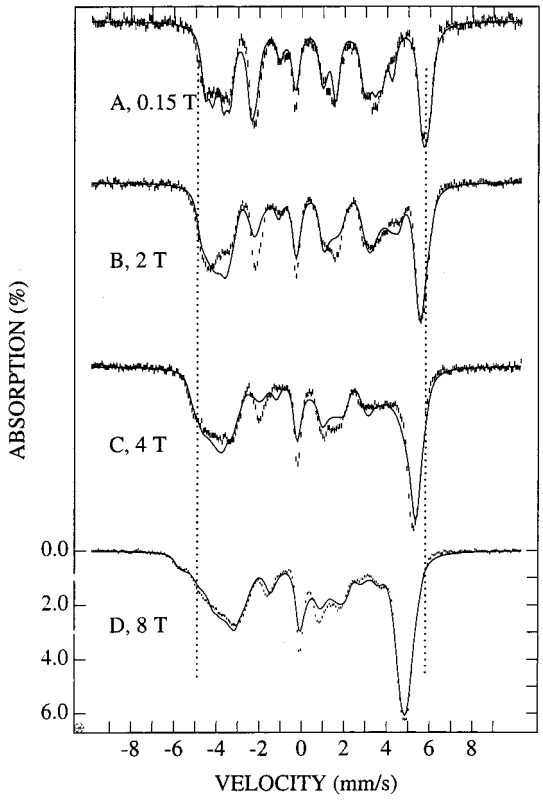

Figure 6. 1.5 K Mössbauer spectrum of Ti(III)citrate-reduced *Av2* recorded in the parallel applied magnetic fields indicated. The solid lines are theoretical spectra computed using the parameters quoted in Table 2.

Therefore, the Mössbauer spectra associated with the φ_1,φ_2 levels exhibit in a 10 mT applied field nearly their full magnetic splittings while those of the φ_3,φ_4 doublet consists of a slightly broadened quadrupole doublet.[26] As can be seen in Figure 5A, the 4.2 K spectrum contains a doublet feature which vanishes when the temperature is lowered to 1.5 K. This feature, shown as a difference spectrum in Figure 5B, has the same pattern as

(25) When the system is quantized along *z*, the φ_1,φ_2 pair is essentially the $M_s = \pm 4$ doublet.

(26) In weak applied fields, the Mössbauer spectra associated with φ_1 and φ_2 are indistinguishable. The same holds for φ_3 and φ_4.

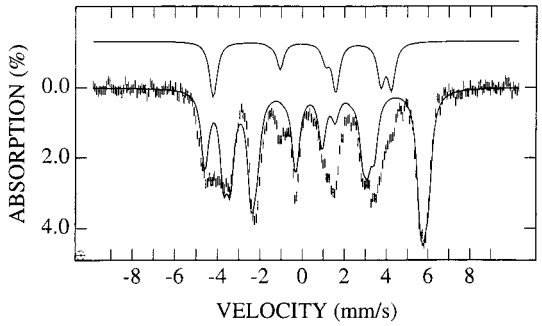

Figure 7. 1.5 K Mössbauer spectrum recorded at a field of 0.15 T applied parallel to the observed γ-radiation (same spectrum as shown in Figure 6A). Solid line drawn through the data shows the contributions of sites 2, 3, and 4. The solid line drawn above the data is the spectrum computed for site 1 (Fe_A).

the spectra of Figure 1, and therefore we assign it to the φ_3,φ_4 levels. A detailed analysis of the 4.2 K spectrum, together with a population analysis of 8 and 15 K data, yields the value $D = -0.75 \pm 0.05$ cm^{-1}. The EPR data analysis yields $\Delta_{ground} = 0.02$ cm^{-1}; this suggests that $E/D = 0.33$.

Figure 6 shows high-field Mössbauer spectra of the [4Fe-4S]^0 cluster recorded at 1.5 K. Because of the small value of D, the φ_3 state is significantly populated at 4.2 K for nearly all applied fields. Since each electronic state contributes four Mössbauer spectra (one for each Fe site), spectral resolution is enhanced at 1.5 K where only the φ_1,φ_2 doublet is populated. For this reason, most spectra were recorded at this temperature. Analysis of the spectra, which may depend on as many as 45 spin Hamiltonian parameters, is described below.

Finally, the Mössbauer data indicate that the Ti(III)citrate-reduced [4Fe-4S] cluster of *Av*2 is essentially 100% in the all-ferrous state; the spectra give no evidence for the presence of [4Fe-4S]$^{2+}$ or [4Fe-4S]$^{1+}$ clusters. However, the shoulder in Figure 1 (arrow) indicates that the sample contains ca. 2% of a high-spin ferrous contaminant.

Analysis of the Mössbauer Spectra. We have analyzed the Mössbauer spectra using the $S = 4$ spin Hamiltonian

$$H = H_e + \sum_{i=1}^{4}\{\mathbf{S}\cdot\mathbf{A}(i)\cdot\mathbf{I}(i) + H_{\mathbf{Q}}(i) - g_N\beta_N\mathbf{B}\cdot\mathbf{I}(i)\} \quad \text{with}$$

$$H_{\mathbf{Q}}(i) = eqV_{\zeta\zeta}(i)/12\ \{3\mathbf{I}_\xi^2 - {}^{15}/_4 + \eta(i)[\mathbf{I}_\xi^2 - \mathbf{I}_\eta^2]\} \quad (2)$$

where $\mathbf{S}\cdot\mathbf{A}(i)\cdot\mathbf{I}(i)$ describes the magnetic hyperfine interactions of the electronic system with the ^{57}Fe nuclei, $H_{\mathbf{Q}}(i)$ describes the interaction of the electric field gradient (EFG, principal axes ξ, η, ζ) tensor with the nuclear quadrupole moment Q and $-g_N\beta_N\mathbf{B}\cdot\mathbf{I}(i)$ is the nuclear Zeeman term. It is unlikely that the tensors describing the local sites coincide with the global frame defined by the zero-field splitting (ZFS) tensor of eq 1. However, to keep the number of unknowns at a manageable level, we have assumed that the A-tensors of sites 2, 3, and 4 are collinear with the ZFS-tensor.

In our analysis we describe the orientation of the quadrupole tensors relative to the ZFS frame by the Euler angles (α_i, β_i, γ_i). Given that D and E/D are known and that the g-tensor of eq 1 is expected to be isotropic within 10% (we have used $g_x = g_y = g_z = 2.0$) we are left with 32 unknowns, namely the hyperfine parameters for each site (A_x, A_y, A_z, sign of ΔE_Q, η, α, β, γ). The problem is further compounded by the fact that the φ_1,φ_2 doublet is magnetically uniaxial for applied fields $B \leq 1$ T. Thus, the expectation values of the electronic spin are highly anisotropic (see Figure 4); e.g. $\langle S_x\rangle = \pm 0.18$, $\langle S_y\rangle = \pm 0.06$ and $\langle S_z\rangle = \pm 3.95$ for the φ_1,φ_2 levels for $B = 0.1$ T. For small B, the internal magnetic fields, $\mathbf{B}_{int}(i) = -\langle\mathbf{S}\rangle\cdot\mathbf{A}(i)/g_N\beta_N$, are fixed relative to the EFG-tensors by the polar angles θ_i and ϑ_i. If $\mathbf{A}(i)$ is collinear with the ZFS-tensor, θ_i and ϑ_i correspond to β_i and γ_i. The low field spectra of each site then depend on $\Delta E_Q(i)$, $\eta(i)$, $|B_{int}(i)|$, θ_i and ϑ_i. It has been shown[27−29] that there exists an infinite manifold of $\{\theta_i, \vartheta_i, \eta(i)\}$ values that yield identical Mössbauer spectra (this *ambiguity problem* has been described in some detail in the analysis of the P-cluster Mössbauer spectra, see ref 27). In strong applied magnetic fields, $\langle S_x\rangle$ and $\langle S_y\rangle$ saturate (Figure 4) and each set of $\{\theta_i, \vartheta_i, \eta(i)\}$ produces distinct spectra; consequently, a parameter set that yields good fits for applied fields of moderate strength may fail to do so for strong fields.

The theoretical curves shown in Figures 3, 6, and 7 were obtained with a computer program that generates Mössbauer spectra after diagonalization of eq 2. This program (WMOSS) allows for least-squares fitting of groups of spectra obtained under different experimental conditions. The fitting option of the program was used in the final stages of spectral analysis in order to refine the parameters of each site. Below we describe a few salient features of the variable-field spectra and establish an association of the spectral features with individual sites.

Sites 2, 3, and 4 have A-tensors with negative components while the unique site, Fe_A, has positive A-tensor components. The following arguments support this statement. The area of the rightmost band in the 0.15 T spectrum (Figure 6A) is fully accounted for by the contribution of three sites. This point is illustrated in Figure 7 which shows, by the solid line drawn through the data, the superposition of spectra simulated for sites 2, 3, and 4. Comparison of the 0.15, 2.0, 4.0, and 8.0 T spectra of Figure 6 (data were also recorded at 1.0, 3.0, and 6.0 T) reveals that the rightmost feature moves uniformly inward with increasing applied fields. This shows that the applied field opposes the internal field, $\mathbf{B}_{int}(i) = -\langle\mathbf{S}\rangle\cdot\mathbf{A}(i)/g_N\beta_N$, at all three sites; i.e., B_{int} is negative. At 1.5 K and $B > 1.0$ T only the φ_1 state is populated; thus, the three components of the spin expectation value, $\langle S_{x,y,z}\rangle$, are negative. An inward movement of the absorption band therefore implies that sites 2, 3, and 4 have negative A-values. Inspection of the spectra in Figure 6 identifies also an outward moving shoulder at the low energy end of the absorption spectrum.[30] Hence, one of the four sites has $A > 0$. Figure 7 suggests that the leftmost line of this component, which we assign to Fe_A, should be positioned at -4.3 mm/s and its rightmost line at $+4.3$ mm/s. We have investigated the possibility of Fe_A contributing to the rightmost band at $+5.8$ mm/s. However, this assignment produced substantially poorer fits.[31]

(27) Zimmermann, R.; Münck, E.; Brill, W. J.; Shah, V. K.; Henzl, M. T.; Rawlings, J.; Orme-Johnson, W. H. *Biochim. Biophys. Acta* **1978**, *537*, 185−207.

(28) Dabrowski, L.; Piekoszewski, J.; Suwalski, J. *Nucl. Instrum. Methods* **1971**, *91*, 93−95.

(29) Torman, J. V. D.; Jagannathan, R.; Trooster, J. M. *Hyperfine Interact.* **1975**, *1*, 135−144.

(30) By following the movement of the leftmost line of Fe_A with increasing applied field, we noted that this line moved, at intermediate fields, with a rate faster than that predicted by the simulations. This suggested that this component may contribute at the left-most edge (at -5 mm/s) of the absorption spectrum. The new assignment, however, creates a pronounced trough between the outward moving line of Fe_A and the inward moving lines of sites 2, 3, and 4, in contrast to the experimental observations. Rotating the direction of the principal component A_z of Fe_A ca. 30° away from the zero-field splitting z-axis towards the x-axis, produces the proper behavior of the left-most line of Fe_A (at intermediate fields the magnetization of the electronic system rotates slightly towards the x-axis where the larger A-value is sampled).

Table 2. Hyperfine Parameters for the $S = 4$ State of the $[4Fe-4S]^0$ State of *Av2*[a]

	site 1 (Fe_A)	site 2	site 3	site 4
δ (mm/s)	0.68	0.68	0.68	0.68
ΔE_Q (mm/s)	−3.08	−1.72	−1.48	1.24
η	1.5	0	0	1.6
β	37.5	56.6	92.3	0
γ	0	4.6	0	90
A_x (MHz)	3(3)	−11.8(8)	−13.7(7)	−13.6(8)
A_y (MHz)	3.4(7)	−10.4(8)	−10(2)	−11(2)
A_z (MHz)	8.6(3)	−11.03	−10.0(3)	−9.6(7)
A_{iso} (MHz)	+5.0(15)	−11.0(7)	−11.4(8)	−11.3(12)

[a] For the simulations we used $D = -0.75$ cm^{-1} and $E/D = 0.33$. α, β, and γ are the Euler angles that rotate the principal axis frame of the local EFG-tensor into the frame of the ZFS-tensor; our simulations suggest $\alpha \approx 0$ for all sites. For site 1 the *z*-axis of the *A*-tensor was rotated by $\beta_A = 30$ degrees relative to the *z*-axis of the EFG-tensor. Numbers in parentheses give estimated uncertainties of the least significant digits.

The solid lines in Figure 6 show the results of our spectral simulations; the parameters used are quoted in Table 2. Given the complexity of the problem, the parameter set fits the experimental spectra remarkably well. However, we have not been able to find a set for Fe_A that is entirely satisfactory; namely, one that properly accounts for the intensity of the weak shoulder at +4.3 mm/s in the spectrum of Figure 6A. We have investigated whether a good fit could be obtained with the 0.15 T spectrum alone (without regards to the high field spectra); however, least-squares fits to this spectrum starting with different sets of initial parameters and component assignments produced results only marginally better than the group fit of Table 2. However, while the numerical values of the *A*-tensor components might have substantial uncertainty, their signs are well known. The conclusion that three sites have negative *A*-values and that one site, *most likely* Fe_A, has positive *A*-tensor components is in accord with the observation that the ground multiplet has electronic spin $S = 4$. We will show below that every $S = 4$ ground multiplet that results from coupling four $S_i = 2$ site spins has this property.

Since the isotropic part of the *A*-tensors, $A_{iso} = (A_x + A_y + A_z)/3$, is most useful for assessing spin coupling models, we have estimated the uncertainties for A_{iso}. This was done by varying the components of the *A*-tensors of each individual site upward and downward until unacceptable fits were obtained. We have also tried different associations for the four iron sites, including association of the $\Delta E_Q = 1.72$ mm/s site with positive *A*-tensor components. While these attempts generated fits of distinctly lesser quality, they yielded A_{iso} values within the quoted limits.

Finally, we would like to discuss the weak-field spectra of Figure 3. The magnetic splittings observed in these spectra arise due to magnetization of the φ_1,φ_2 levels along the *z* direction, as shown in the inset of Figure 4.[25] The slope of these magnetization curves depend critically on Δ_{ground}, and thus the low-field spectra can be used to determine the value of this parameter. The solid lines in Figure 3A and B are theoretical curves obtained from the parameter set of Table 2 for $\Delta_{ground} = 0.015$ and 0.03 cm^{-1}. It can be seen that $\Delta_{ground} = 0.03$ cm^{-1} does not produce a sufficiently large splitting. On the other hand, $\Delta_{ground} = 0.015$ cm^{-1} generates a spectrum with sufficient splitting but too much intensity in the outermost bands. These observations show that the value of Δ_{ground} is between 0.03 and 0.015 cm^{-1}.

(31) Under conditions where the electronic spin relaxes fast compared to the nuclear precession frequencies, one can determine the sign of the *A*-values for Fe_A from studies in strong applied magnetic fields. However, even at 200 K the relaxation rate of the $S = 4$ system is not fast enough to permit such studies.

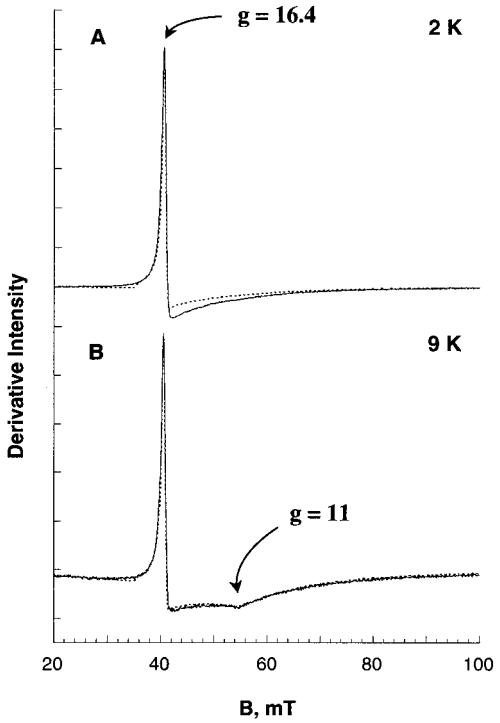

Figure 8. Parallel mode EPR spectra of Ti(III)citrate-reduced *Av2* recorded at 2 K (A) and 9 K (B). Dashed lines are quantitative spectral simulations produced with the following parameters: $g_x = 2.0$ and $g_y = g_z = 2.05$, $D = -0.8$ cm^{-1}, $\gamma_E = -0.254$ cm^{-1}, $\sigma_E = 0.06$ cm^{-1}, and $\sigma_B = 0.25$ mT. Spectra shown were obtained with the same sample used for Figures 9, 10, and 11. Protein concentration was 2.1 mM. Instrumental conditions: microwaves, 0.2 mW, 9.27 GHz; modulation, 0.49 mT, 100 kHz. Spectra are not sensitive to g_x.

Comparison of the simulations of Figure 3A and B suggests that the sample contains an ensemble of molecules with different Δ_{ground}-values. This distribution in electronic parameters was also inferred from analysis of the EPR data (see below) which could be fit by assuming that the ZFS parameter *E* has a Gaussian distribution with $\sigma_E = 0.06$ cm^{-1}. Because $\Delta_{ground} = 2.2D(E/D)^4$, a distribution in *E* entails a distribution in Δ_{ground}. The solid lines of Figure 3C and D are simulations produced using the parameters of Table 2 with $\Delta_{ground} = 0.02$ cm^{-1} and the distribution that fits the EPR spectra. While the simulations suggest that a Gaussian distribution in *E* is not entirely correct, they capture the essential features of the spectra.

EPR Studies. The energy level scheme of Figure 2 drawn for the ZFS parameters obtained in the previous section suggests that X-band EPR spectra of the all-ferrous cluster should display a variety of integer spin signals. Indeed, we have observed resonances arising from four doublets of the $S = 4$ multiplet, as indicated in Figure 2. Figure 8A and B show parallel mode X-band spectra recorded at 2 and 9 K, respectively. The 2 K spectrum exhibits a sharp resonance (ca. 0.7 mT width) at $g = h\nu/\beta\mathbf{B} = 16.4$ which we assign to a transition between the levels of the φ_1,φ_2 doublet. At 9 K (Figure 8B), a second broader feature appears around $g \approx 11$ which we assign to levels φ_3 and φ_4. As the temperature is raised above 9 K, additional signals resulting from transitions between other members of the $S = 4$ manifold are also observed (see below).

A component of the applied magnetic field along the *z*-axis of the ZFS-tensor will split the φ_1,φ_2 and φ_3,φ_4 doublets by an

energy

$$\delta E = \sqrt{\Delta^2 + (2\beta g_{\text{eff}} B_z)^2}$$

where Δ is the zero-field splitting for each doublet. For $E/D = {}^1/_3$, the effective g-value for the ground doublet is $g_{\text{eff}} = 2Sg_z = 8g_z$; for the φ_3,φ_4 doublet $g_{\text{eff}} = 5.5\ g_z$ is expected for the same E/D value. The observed g-values, $g = h\nu/\beta\mathbf{B}$, will differ from g_{eff} due to Δ and the asymmetry of the line shape. The observed g-values at $g = 16.4$ and 11 are close to the predicted values for $g_z \approx 2$ and thus suggest that the resonances belong to an $S = 4$ multiplet.

Simulations generated for an $S = 4$ system with $D = -0.8$ cm^{-1} and $E/D = 0.32$ (these parameters yield $\Delta_{\text{ground}} = 0.02$ cm^{-1}) are shown as the dashed lines in Figure 8. The good match between theory and experiment provides unambiguous evidence that the observed signals are indeed associated with a $S = 4$ system. Simulations using any other spin multiplet do not reproduce both the proper line positions and signal intensities. Moreover, the ZFS parameters used are in good agreement with the values obtained from Mössbauer spectroscopy. Quantitation of the signal based on these simulations gave a value for the spin concentration that was 20% less than the measured protein concentration.

In the rhombic limit ($E/D = {}^1/_3$), the $S = 4$ system displays symmetries that can be used to determine both g_y and g_z. For $E/D = {}^1/_3$, the Hamiltonian of eq 1 predicts that the members of the uppermost doublet (φ_8,φ_9) will be split by the same Δ as the φ_1,φ_2 doublet. Thus, an EPR resonance arising from transitions within the φ_8,φ_9 doublet should be observed at g_{eff} (upper doublet) $= g_{\text{eff}}$ (ground doublet)g_y/g_z when the static magnetic field is along the molecular y-axis. We have recorded variable temperature spectra over a narrow field range centered around g = 16.4 (data not shown) and observed that the resonance broadens by ~0.2 mT to higher fields at temperatures above 16 K. Thus, g_y and g_z must be approximately equal; from the simulations these values were determined to be $g_y \approx g_z \approx 2.05$.

The $g = 16.4$ ground resonance is observed in a field region where $g_{\text{eff}}\beta\mathbf{B} \gg \Delta_{\text{ground}}$; thus, the position of this feature depends critically on g_{eff} but very little on Δ_{ground} (a 50% change of Δ_{ground} will shift the resonance by only 0.05 mT). In contrast, the EPR spectrum resulting from transitions within the φ_3,φ_4 doublet is very sensitive to variations in Δ_{exc}. The broad features emerging at 9 K (Figure 8B) suggest that Δ_{exc} is distributed for the ensemble of molecules in the frozen sample (see shaded areas in Figure 2). We have modeled this distribution by assuming that the ZFS parameter E has a Gaussian distribution around a mean value of $\bar{\Delta}_{\text{exc}} = -0.254$ cm^{-1} with width $\sigma_E = 0.06$ cm^{-1}. A distribution with $\sigma_E = 0.06$ cm^{-1} also improves the simulation of the 2 K spectrum, especially in the low-field tail of the $g = 16.4$ resonance. We have assumed for all simulations Gaussian spin packets of width $\sigma_B = 0.25-0.68$ mT.[32]

For $E/D = {}^1/_3$, the φ_6,φ_7 doublet has the same splitting as the φ_3,φ_4 doublet, and both pairs of levels will yield the same EPR features, with intensities governed by the respective Boltzmann factors. The simulation shown in Figure 9A was generated with a program that takes into account the Boltzmann populations of the various levels (as described in the Materials and Methods section); this simulation thus contains contributions of resonances arising from four doublets. The inset in Figure 9A shows the spectra of each of the four levels weighted according to their Boltzmann factors. The parameters used for the simulations are listed in the caption of Figure 9. It should be noted that $\bar{\Delta}_{\text{exc}} = 0.44$ cm^{-1} is larger than the X-band microwave quantum, i.e., the excited-state spectrum results from those molecules (~20%) that are at the low end of the Δ_{exc} distribution (see ref 24).

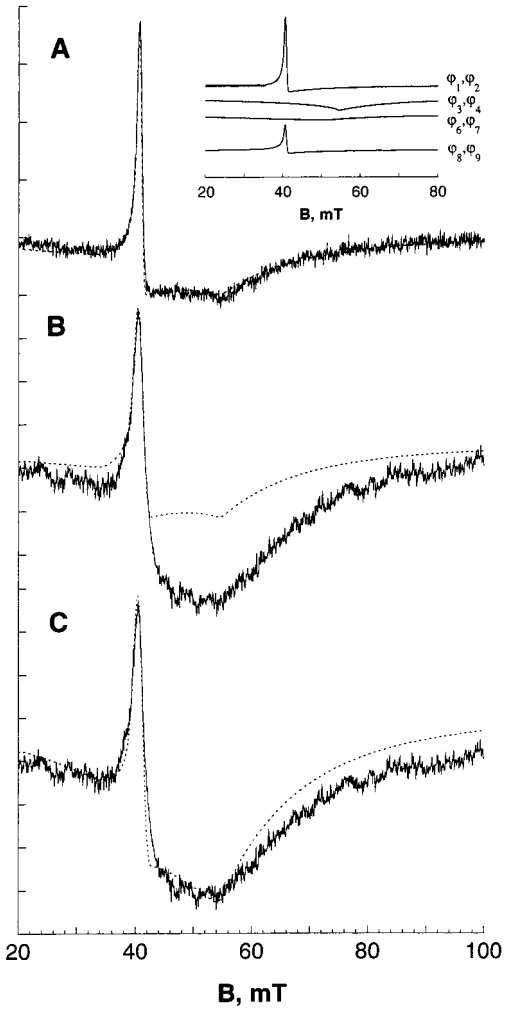

Figure 9. Parallel mode EPR spectra recorded at 40 K (A) and 120 K (B,C). Dashed lines of (A) and (B) are simulations of the ground $S = 4$ multiplet signal; (C) contains an additional 55% contribution of a resonance arising from an $S = 3$ excited spin multiplet (see text). Inset shows the resonances of the (φ_1,φ_2), (φ_3,φ_4), (φ_6,φ_7), and (φ_8,φ_9) doublets (from top to bottom) weighted according to the appropriate Boltzmann factors. Spin packet line widths were adjusted[32] to $\sigma_B = 0.32$ mT for (A) and $\sigma_B = 0.68$ mT for (B,C); all other parameters were fixed to the values quoted in the caption of Figure 8. Instrumental conditions: microwaves, 0.2 mW (A) and 20 mW (B, C), 9.27 GHz; modulation, 0.49 mT, 100 kHz. Spectra shown in (A) and (B,C) were signal-averaged for 22 and 11 min, respectively.

The $g = 16.4$ resonance can be observed quite well at temperatures up to 140 K. Because the ZFS parameters of the $S = 4$ multiplet are known from the studies described above, one can readily compute the intensity of the $g = 16.4$ resonance (s) as a function of temperature. Comparison of the predicted intensities to the experimentally observed ones would reveal whether multiplets other than the $S = 4$ state become measurably populated at temperatures below 140 K.

The variable temperature spectra, recorded at 2, 10, 16, 24, 39, 51, 67, 80, 96, 109, and 122 K, were analyzed by integrating the EPR spectra and evaluating the area under the $g = 16.4$

(32) Line widths of the spin packets (σ_G)were increased for $T \geq 40$ K in order to account for lifetime broadening.

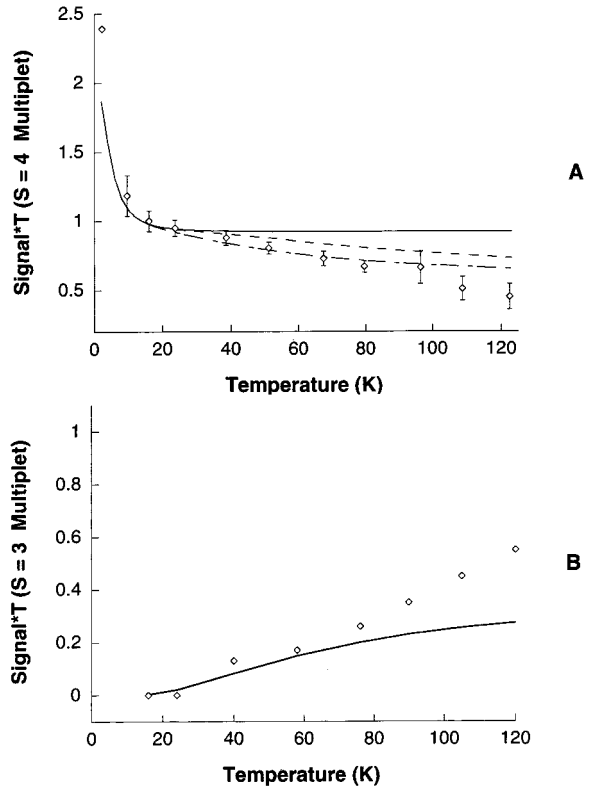

Figure 10. (Signal**T*) vs. *T* plot for ground (A) and excited (B) spin multiplets. Solid line, dashed line and dots and dashes in (A) are theoretical curves computed for the cases where the ground $S = 4$ multiplet is separated from excited spin multiplets by $\Delta E = \infty$, 100 and 60 cm^{-1}, respectively. Solid line in (B) is a theoretical curve computed assuming an $S = 3$ multiplet at energy $E = 60$ cm^{-1}. The plots shown in (A) and (B) result from the analysis of different sets of EPR data collected for the same sample. We have not included an error bar for the 2 K data point in (A) because we have not studied temperature gradients in sufficient detail.

feature. The results, including estimated uncertainties, are plotted in Figure 10A as a (Signal**T*) vs *T* plot. The solid line is a theoretical curve computed with the assumption that the $S = 4$ multiplet is well separated in energy ($\Delta E = \infty$) from excited spin multiplets. In contrast to the experimental data, the theoretical curve predicts that the quantity (Signal**T*) remains constant at temperatures above 40 K. This discrepancy suggests that low-lying excited spin multiplets are accessible over the temperature range sampled.[33]

Analysis of the spin-coupling model of the all-ferrous cluster, presented below, suggests that the first excited spin manifold has $S = 3$. To assess the energy of such an $S = 3$ state, we have computed the intensity of the $g = 16.4$ resonance as a function of temperature assuming that an $S = 3$ manifold is present at energy ΔE, taking into account the measured ZFS of the ground multiplet but setting $D = 0$ for the $S = 3$ manifold. Two theoretical curves, computed for $\Delta E = 100$ cm^{-1} (dashed line) and $\Delta E = 60$ cm^{-1} (dots and dashes), are shown in Figure 10A. While the $\Delta E = 60$ cm^{-1} curve describes the data quite well up to 100 K, above this temperature the experimental data seem to fall off more rapidly than predicted by the simple model. Perhaps, one could improve the agreement between theory and experiment by allowing a second excited state to become populated. The all-ferrous cluster has 84 excited spin multiplets belonging to the orbital ground state.

We have simulated the spectra of the $S = 4$ multiplet over the experimental temperature range. Comparison of the experimental $g = 16.4$ intensities with those predicted from the simulations allowed for an independent measure of the population in the $S = 4$ multiplet as a function of temperature. This analysis yielded, within the uncertainties, the same data points as plotted in Figure 10A. The good agreement between the two methods used to analyze the temperature dependence of the population of the ground multiplet suggests that the data are not afflicted by systematic errors.

While the simulations match the experimental data exceedingly well up to 40 K (Figure 9A), at higher temperatures they fail to reproduce the intensity of the broad $g = 11$ resonance (Figure 9B). We wondered whether this mismatch could be attributed to a resonance originating from a low-lying $S = 3$ multiplet. Such a multiplet can produce, for its $M_s = \pm 3$ doublet, resonances whose shapes depend on the Δ-value ($\Delta_{S=3}$) of the doublet and the distribution of $\Delta_{S=3}$. Within the uncertainties, the resonance emanating from the $S = 3$ multiplet, seems to have a shape similar to that originating from the φ_3,φ_4 doublet of the $S = 4$ multiplet. For the quasi-doublets encountered here, the shape of the EPR spectrum depends essentially on $\bar{\Delta}$ and its distribution. Therefore, we have simulated this spectrum resulting from the $S = 3$ multiplet by assuming $\bar{\Delta}_{S=3} = \bar{\Delta}_{exc}$ and applying the same distribution as used for the ground multiplet. A simulation for the 120 K spectrum is shown in Figure 9C (parameters are quoted in the figure caption), for which we have assumed that 55% of the all-ferrous clusters are in the $S = 3$ excited state. Using this procedure we have estimated the population of the $S = 3$ multiplet as a function of temperature; this yielded the (Signal**T*) vs *T* plot (for the $S = 3$ multiplet) shown in Figure 10B. It is important to note that the fraction of clusters in the excited spin manifold (Figure 10B) correlates well with the fractional depopulation of the ground $S = 4$ ground multiplet (Figure 10A), inferred from matching the simulations to the $g = 16.4$ resonance. On the other hand, the data suggests that at 120 K (Figure 9C) approximately 55% of the clusters are in the excited spin manifold; this fraction indicates that a two-multiplet model may be oversimplified and that the cluster must thus be able to access other higher lying spin multiplets at this temperature.

X-ray Radiolytic Reduction of the [4Fe-4S]$^{1+}$ Cluster at 77 K. Given that the [4Fe-4S] cluster of *Av2* is bound to the interface of an α_2 protein dimer, we were surprised to observe that one site, Fe_A, has a ΔE_Q-value distinctly different from those of the other three sites. We have not detected any nucleotide in the ^{57}Fe Fe protein using a high performance liquid chromatography method;[35] moreover, we have also shown that the Mössbauer spectrum of the all-ferrous [4Fe-4S] cluster does not change upon the addition of MgATP.[14] Another concern was that excess citrate, present in solutions of the Ti(III)citrate reductant, could bind to the Fe protein, produce a distortion, and thereby cause the 3:1 asymmetry. However, deazariboflavin-reduced (Figure 11A, solid line), bisaquo (1,4,8,12-tetraazacyclopentadecanyl)-Cr(II)-reduced (data not shown) and Ti(III)-citrate-reduced (Figure 11A, dashed line) *Av2* display identical $S = 4$ EPR signals. The X-ray structure of *Av2*[2,3] has shown that the cluster is coordinated by four cysteinyl sulfurs. To test

(33) The temperature dependence of ΔE_Q (Table 1) implicates the presence of a low-lying excited orbital state; we have used the model developed by Bertrand and Gayda[34] and estimated that the excited state is separated from the ground state by at least 250 cm^{-1}.

(34) Bertrand, P.; Gayda, J.-P. *Biochim. Biophys. Acta* **1979**, *579*, 107−121. (b) Bertrand, P.; Guigliarelli, B.; Gayda, J.-P.; Beardwood, P.; Gibson, J. F. *Biochim. Biophys. Acta* **1985**, *831*, 261−266.

(35) Stocchi, V.; Cucchiarini, L.; Magnani, M.; Chiarantini, L.; Palma, P.; Crescentini, G. *Anal. Biochem.* **1985**, *146*, 118−124.

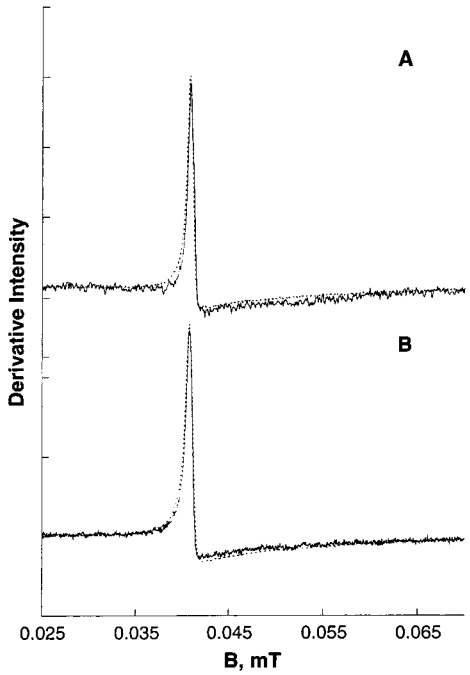

Figure 11. Parallel mode EPR spectra of Ti(III)citrate-reduced (A and B, dashed lines), deazariboflavin-reduced (A solid line), and radiolytically reduced (B, solid line) *Aυ2*. Protein data for deazariboflavin-reduced sample: 0.16 mM, 0.2 mM 5′-deazariboflavin, 2mM EDTA. Protein data for irradiated sample: 0.19 mM, 10% v/v glycerol. Instrumental conditions: 2 K; microwaves, 1.26 mW, 9.27 GHz; modulation, 0.49 mT, 100 kHz.

whether the coordination environment of one cluster site, namely Fe_A, changes upon reduction to the all-ferrous state, we have attempted a radiolytic reduction of dithionite-reduced [4Fe-4S]$^{1+}$ Fe protein in a synchrotron X-ray beam at 77 K (see Materials and Methods). Figure 11B shows that the γ-irradiation not only produces an all-ferrous state, but it produces the same state as the one obtained by chemical reduction with Ti(III)citrate. Comparison of the $S = 4$ signal intensity of the radiolytically reduced sample to that of a sample of known [4Fe-4S]^0 concentration indicates that ca. 60% of the clusters were reduced to the all-ferrous form. Because the Fe protein was irradiated at 77 K and stored in liquid nitrogen before examination at 2 K by EPR, ligand exchange after reduction is exceedingly improbable.

A Spin-Coupling Model for the All-ferrous State. In this section we discuss a spin-coupling model aimed at exploring the conditions that give rise to an $S = 4$ ground state. We assume that the four high spin ($S_i = 2$) sites of the all-ferrous cluster are antiferromagnetically coupled by isotropic exchange interactions

$$H_{ex} = \sum_{i<j} J_{ij} \mathbf{S}_i \cdot \mathbf{S}_j \qquad (3)$$

The Hamiltonian of eq 3 produces 85 spin multiplets, 15 of which have total spin $S = 4$. Because the exchange interactions are assumed to be isotropic, the system spin S is a good quantum number; however, the Hamiltonian mixes multiplets with the same spin.

High-spin $Fe^{2+}S_4$ sites have formidable zero-field splittings; Fe^{2+}-rubredoxin, for instance, has $D \approx 8$ cm^{-1}.[23] Since the ZFS terms of the individual sites, $\mathbf{S}_i \cdot \mathbf{D}_i \cdot \mathbf{S}_i$, do not commute with the Hamiltonian of eq 3, multiplets with $S \neq 4$ can mix into the ground multiplet and thus lead to states with mixed-spin character. Because eq 3 contains already six unknown J-values, and because we have no information on the magnitudes and orientations of the individual D_i-tensors, we will neglect zero-field splittings in our model.

Although the [4Fe-4S] cluster of the Fe protein is suspended at the interface of an α_2 protein dimer, the Mössbauer and EPR data do not provide any evidence for the presence of a 2-fold (or nearly 2-fold) symmetry. This lack of symmetry is particularly pronounced for the ΔE_Q-values of this cluster, which occur in an approximate 3:1 ratio. For these reasons, we have not assumed in our model any symmetries other than those following from the permutation of the site indices.

We have solved eq 3 by computer diagonalization of the subspaces belonging to multiplets with the same total spin S. The matrix elements were computed in the basis $|(S_1S_2)S_{12}(S_3S_4)S_{34};S,M_s = 0\rangle$ using the operator algebra outlined by Bencini and Gatteschi.[36] These authors have given expressions (their eqs 4.35 and 4.36) that are particularly suitable for setting up matrix elements of a 4-spin problem. The program was debugged at the final stages by two independent checks: (i) The energies of the 85 spin multiplets were calculated for a set of J-values followed by systematic permutation of the site indices; (ii) The energies and spin projection factors were calculated for J-values for which an exact solution is known.

For a given set of J-values we have computed the energies of all multiplets resulting from eq 3, retaining only those sets that produce an $S = 4$ ground state. We have computed the relative energies of the multiplets by keeping one J-value fixed and scaling relative to this coupling constant. Without loss of generality one can assume that the fixed J-value, J_{14} in our case, is the largest one. In our calculations we have varied the five other J-values from zero to J_{14} in steps of $J_{14}/10$. Because there are no reported cases of ferromagnetic coupling in iron−sulfur clusters, we kept all J-values positive. For every solution yielding an $S = 4$ ground multiplet we computed the spin projection factors K_i ($i = 1-4$) that relate the magnetic hyperfine tensors of eq 2, $\mathbf{A}(i)$, to the intrinsic tensors, $\mathbf{a}(i)$, of each iron site; $\mathbf{A}(i) = K_i\mathbf{a}(i)$.[37] Not surprisingly, the calculations indicate that $S = 4$ ground states can result for a broad range of J-value sets, although all solutions share common features. Every solution produces one negative and three positive spin projection factors, i.e., the occurrence of one positive and three negative A-values is a property of every $S = 4$ ground multiplet.

The essential features of the solutions are illustrated in Figure 12. Scheme A shows a symmetric case with $J_{12} = J_{13} = J_{14} = J$, $J_{23} = J_{34} = J'$, and $J_{24} = J''$; for this case the Hamiltonian of eq 3 can be solved exactly in the $|S_{24}S_{243};S,M_s = 0\rangle$ representation where $\mathbf{S_{24}} = \mathbf{S_2} + \mathbf{S_4}$, $\mathbf{S_{243}} = \mathbf{S_{24}} + \mathbf{S_3}$ and $S = \mathbf{S_1} + \mathbf{S_{243}}$. It is readily understood that an $S = 4$ ground-state results for $J \gg J', J''$. For these conditions, the strong antiferromagnetic couplings that link site 1 with sites 2, 3, and 4 orient $\mathbf{S_2}$, $\mathbf{S_3}$, and $\mathbf{S_4}$ antiparallel to $\mathbf{S_1}$; for maximal antiparallel alignment, $S_{243} = 6$ combines with $S_1 = 2$ to yield a system spin $S = 4$. One can proceed to lower symmetry by allowing $J_{23} \neq J_{34}$ and decreasing J_{13} (Scheme B). As J_{13} is lowered, the spin alignment is maintained as long as the sum $J_{23} + J_{34}$ is adjusted to values such that $\mathbf{S_3}$ is not reoriented in a significant way. Similar arguments hold at the node of site 2 when J_{12} is varied.

Inspection of the entire solution set revealed a significant result, namely that the various iron pairs have J-values that differ substantially. The all-ferrous cluster must contain two J-values

(36) Bencini, A.; Gatteschi, D. In *EPR of Exchange Coupled Systems*; Springer-Verlag: Berlin, 1990; Chapter 4.

(37) Mouesca, J.-M.; Noodleman, L.; Case, D. A.; Lamotte, B. *Inorg. Chem.* **1995**, *34*, 4347−4357.

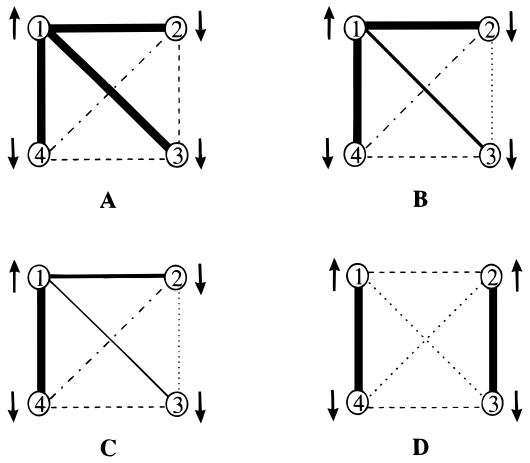

Figure 12. Coupling diagrams illustrating occurrence of $S = 4$ ground states for the all-ferrous cluster. Strength of the exchange couplings, assumed to be antiferromagnetic, is indicated by the thickness of the lines connecting the sites. Broken lines indicate weaker interactions. At sites 2 and 3 the inequalities $J_{23} + J_{24} < 0.75\ J_{12}$ and $J_{23} + J_{34} \leq 0.75\ J_{13}$ have to be fulfilled. Case D cannot produce an $S = 4$ ground state.

that differ in magnitude by at least a factor 3, $J_{max}/J_{min} \geq 3$. The equality holds for the rather symmetric case $J_{12} = J_{13} = J_{14} = J$ and $J_{23} = J_{24} = J_{34} = J'$ for which eq 3 solves as $E = JS(S + 1) - (J - J')S_{243}(S_{243} + 1)$ yielding an $S = 4$ ground multiplet for $J'/J < {}^1/_3$. Moreover, inspection of the computer-generated solutions revealed that in order to have an $S = 4$ ground state, the inequalities $J_{24} + J_{23} \leq 0.75J_{12}$ and $J_{23} + J_{34} \leq 0.75J_{13}$ must be fulfilled at the nodes of sites 2 and 3, respectively; this implies that there must be two additional J-values (not including J_{max} and J_{min}) that differ by at least a factor 2.5. Fulfillment of the above conditions is necessary but not sufficient for the occurrence of an $S = 4$ ground state. We have found that a few isolated J-sets, present at the boundaries of a contiguous $S = 4$ solution space, satisfy the node conditions and yet lead to ground states with $S = 3$, 2, or 1. Furthermore, the numerical analysis showed that every $S = 4$ ground state is accompanied by a first excited state with $S = 3$. The principal types of $S = 4$ solutions are illustrated in schemes A−C of Figure 12. Scheme D illustrates a case (C_2 symmetry) that does not yield an $S = 4$ ground state.

For systems containing only high-spin ferric ions[38] or for the fairly straightforward case of [2Fe-2S]$^+$ clusters,[39] one can evaluate the spin projection factors K_i reasonably well from the observed magnetic hyperfine couplings. The K_i-values, in turn, can give insight into the coupling scheme and information on the ratios of the J-values.[38] For the all-ferrous state this procedure is less straightforward. Since three principal axis values of the A-tensors need to be determined, there are substantial experimental uncertainties associated with these parameters. By averaging the principal axis components of the ferrous A-tensor, the traceless spin-dipolar contribution cancels. The resulting A_{iso}-values, $A_{iso}(i) = K_i a_{iso}(i)$, however, contain a contact contribution, $a_c(i)$, and a pseudo-contact term, $a_l(i)$, the latter resulting from an orbital contribution [$a_{iso}(i) = a_c(i) + a_l(i)$]. The quantity $a_l(i)$ is proportional to Tr($\Delta\mathbf{g}(i)$), where $\Delta\mathbf{g}(i) = \mathbf{g}(i) - 2$ and $\mathbf{g}_i$ is the g-tensor of site i (For a detailed discussion the reader is referred to the analysis of Mouesca et al.[37]). Because $\mathbf{g}_i(i)$ is related to the ZFS-tensor of the ferrous ion,[40] the value of $a_{iso}(i)$ of the all-ferrous cluster is affected by the unknown zero-field splitting of site i. The orbital contribution to $a_{iso}(i)$ can be sizable; for example, for ferrous rubredoxin[37] $a_c(Fe^{2+}) \approx -31.4$ MHz and $a_l(Fe^{2+}) \approx +9.0$ MHz combine to yield the experimentally observed $a_{iso}(Fe^{2+}) = -22.4$ MHz.

The exact solution quoted above yields $K_1 = -{}^2/_5$ and $K_2 = K_3 = K_4 = {}^7/_{15}$. Using $a_{iso}(Fe^{2+}) = -22.4$ MHz we obtain $A_{iso}(2) = A_{iso}(3) = A_{iso}(4) = -10.5$ MHz, in satisfactory agreement with the experimental values of −11.0, −11.4, and −11.3 MHz for sites 2, 3, and 4. On the other hand, the same $a_{iso}(Fe^{2+})$ yields $A_{iso}(1) = +9.0$ MHz, which is substantially larger than $A_{iso}(1) = +(5.0 \pm 1.5)$ MHz obtained experimentally for Fe_A.

Our calculations show that none of the computer-generated solutions of eq 3 produce a set of K_i-values that fits the data for one value of $a_{iso}(Fe^{2+})$. Because $\sum_i K_i = 1$ and because $K_1 < 0$, the desired reduction of K_1 requires that at least one of the other K-values is reduced by a similar amount, leading to a mismatch for $A_{iso}(2)$, $A_{iso}(3)$, and $A_{iso}(4)$. Analysis of the [2Fe-2S]$^+$ data[37] suggests $a_{iso}(Fe^{2+}) = -16.5$ MHz for the ferrous site. This value would yield, for $K_1 = -{}^2/_5$, a reasonably satisfactory $A_{iso}(1) = 6.6$ MHz, but would produce too small A_{iso} values for the other three sites. Thus, our experimental data cannot be explained by assuming that all sites of the all-ferrous cluster have the same intrinsic a_{iso}-values.

In summary, our analysis suggests the following features of the all-ferrous cluster:

(i) The six J-values of the cluster must have substantially different magnitudes. Two J-values must obey the inequality $J_>/J_< \geq 3$ and two other J-values must obey $J_>/J_< \geq 2.5$.

(ii) The two largest J-values must involve site 1 whose spin is oriented antiparallel to the cluster spin S. Our analysis suggests that site 1 corresponds to Fe_A, the site exhibiting the large ΔE_Q-value, $\Delta E_Q = 3.08$ mm/s at 4.2 K.

(iii) All J-value sets that produce an $S = 4$ ground multiplet yield a first excited state with $S = 3$.

(iv) The observed magnetic hyperfine couplings cannot be explained for any J-value set if one assumes that all four sites have the same intrinsic a_{iso}-values.

(v) C_2 cluster symmetry does not produce $S = 4$ ground states.

Discussion

We have studied here with Mössbauer and EPR spectroscopy the Ti(III)citrate-reduced Fe protein from *Azotobacter vinelandii*. The isomer shifts and quadrupole splittings observed for the four Fe sites unambiguously establish that the [4Fe-4S] cluster is in the all-ferrous state. An all-ferrous state implies that the cluster spin should be integral or zero, in accord with the observation of integer-spin EPR signals belonging to an $S = 4$ spin system. Perhaps most surprising to us was the observation that one Fe site, Fe_A, has ΔE_Q-values (Table 1) significantly larger than those observed for the other three sites. Given that the cubane cluster of *Av2* is suspended at the interface of an α_2 protein dimer, one would expect the four sites of the all-ferrous cluster to occur with a 2:2 (perhaps with a minor distortion toward lower symmetry) occupation ratio. Musgrave et al. have recently reported an EXAFS study of all-ferrous *Av2*.[41] The best fits to their data were obtained using four short (2.53 Å) and two long (2.77 Å) Fe−Fe distances, a metric compatible with

(38) Kent, T. A.; Huynh, B. H.; Münck, E. *Proc. Natl. Acad. Sci. U.S.A.* **1980**, *77*, 6574−6576.

(39) Münck, E.; Debrunner, P. G.; Tsibris, J. C. M.; Gunsalus, U. C. *Biochem.* **1972**, *11*, 855−863. (b) Fritz, J.; Anderson, R.; Fee, J.; Petering, D.; Palmer, G.; Sands, R. H.; Tsibris, J. C. M.; Gunsalus, I. C.; Orme-Johnson, W. H.; Beinert, H. *Biochim. Biophys. Acta* **1971**, *253*, 110−133.

(40) Abragam, A.; Bleaney, B. In *Electron Paramagnetic Resonance of Transition Ions*; Dover Pub., Inc.: New York, 1970; Chapter 19.

(41) Musgrave, K. B.; Angove, H. C.; Burgess, B. K.; Hedman, B.; Hodgson, K. O. *J. Am. Chem. Soc.* **1998**, *120*, 5325−5326.

Table 3. ΔE_Q and δ-Values, at 4.2 K, of *Av2* and High-Potential Iron Protein (HiPIP) from *C. Vinosum*[a]

	pair I			pair II		
oxidation state		δ (mm/s)	ΔE_Q (mm/s)		δ (mm/s)	ΔE_Q (mm/s)
Av2, 0	$Fe^{2+}Fe^{2+}$	0.68	1.24, 3.08[a]	$Fe^{2+}Fe^{2+}$	0.68	1.48, 1.72[a]
Av2, 1+	$Fe^{2.5+}Fe^{2.5+}$	0.53	0.98	$Fe^{2+}Fe^{2+}$	0.59	1.60
Av2, 2+	$Fe^{2.5+}Fe^{2.5+}$	0.45	1.22	$Fe^{2.5+}Fe^{2.5+}$	0.45	1.22, 0.83
HiPIP, 2+	$Fe^{2.5+}Fe^{2.5+}$	0.40	1.14	$Fe^{2.5+}Fe^{2.5+}$	0.43	1.14
HiPIP, 3+	$Fe^{3+}Fe^{3+}$	0.29	0.88	$Fe^{2.5+}Fe^{2.5+}$	0.40	1.03

[a] Assignment of the ΔE_Q-values to pairs I and II is arbitrary. Moreover, there is no evidence that the four sites of the all-ferrous state can fruitfully be grouped in pairs.

a tetragonally compressed structure. The approximate 3:1 ΔE_Q ratio (the ΔE_Q-values of three sites are similar but not identical) determined by Mössbauer spectroscopy suggests a cluster symmetry lower than anticipated from the protein symmetry and the EXAFS analysis. A lower symmetry is also indicated by the observation that the electronic ground state has spin $S = 4$. The spin-coupling model discussed above reveals that a cluster with C_2 symmetry cannot yield a ground state with $S = 4$. Moreover, our analysis shows that all possible $S = 4$ ground multiplets of an all-ferrous cluster must have one site with a negative spin projection factor K_1 and three sites with positive factors; the best fits to the Mössbauer data suggest that Fe_A, the component with the largest ΔE_Q, is associated with K_1.

The metal center of *Av2* is the first [4Fe-4S] cluster that has been stabilized, without the use of chaotropic agents,[18] in three stable core oxidation states. It will thus be instructive to discuss briefly the changes in isomer shifts between the different oxidation states.[42] It is well-established that the isomer shift is a good indicator of the oxidation state of an iron site. Although δ is a measure of the s-electron density at the nucleus, this quantity, because of shielding effects, is also a good measure of the 3d electron population.[44] A wealth of spectroscopic data has established that the iron sites of [4Fe-4S] cubanes can be grouped in pairs.[43,45] For instance, in the 3+ oxidation state the cluster contains an $Fe^{3+}Fe^{3+}$ pair and a mixed valence (MV) $Fe^{2.5+}Fe^{2.5+}$ pair. Addition of one electron yields the 2+ state which comprises two MV pairs. Upon further reduction by one electron, the cluster attains the 1+ state which, in the $S = {}^1/_2$ form, exhibits a MV pair and an $Fe^{2+}Fe^{2+}$ pair. Table 3 lists ΔE_Q- and δ-values of the clusters of *Av2*[46] and the high-potential iron protein (HiPIP) from *Chromatium vinosum*.[47] All protein-bound [4Fe-4S] clusters exhibit in the 2+ state, within a narrow margin, δ-values near 0.45 mm/s. The diferrous pair of the 1+ state has $\delta = 0.59$ mm/s, a value that is about 0.09 mm/s smaller than the "saturation" value of 0.68 mm/s observed for the all-ferrous state. The missing 3d-electron density seems to have migrated from the diferrous pair to the MV pair, whose shift has increased by 0.08 mm/s relative to its value in the 2+ state. A similar, but less pronounced trend is observed for the HiPIP cluster, for which the $Fe^{3+}Fe^{3+}$ pair has reached a value of 0.29 mm/s; this value is 0.05 mm/s larger than the δ-value of Fe^{3+}-rubredoxin.[48] It thus appears that in oxidized HiPIP some d-electron density has been transferred from the MV pair to the diferric pair.

The question arises as to whether Fe_A is already special in the 1+ oxidation state. Previous Mössbauer studies indicated that the $[4Fe\text{-}4S]^{1+}$ cluster (see Table 3) contains a mixed-valence pair with $\Delta E_Q = 0.98$ mm/s and a diferrous pair with $\Delta E_Q = 1.6$ mm/s; thus, a component with $\Delta E_Q \approx 3$ mm/s is absent in this cluster state. However, it is possible that, in the 1+ state, Fe_A belongs to the mixed valence pair. For mixed valence pairs the orbital ground states of the two iron sites can be modified by the presence of a strong resonance delocalization interaction[50] and, moreover, the electric field gradients of the two sites are averaged, producing the $\Delta E_Q = 0.98$ mm/s observed for each site of the pair. Thus, an Fe_A-type site belonging to the MV pair of the 1+ state could be masked by the effects of resonance interactions. Alternatively, formation of a site like Fe_A may be an intrinsic feature of the electronic structure of the $[4Fe\text{-}4S]^0$ core. It is interesting to note that the X-ray structure of *Av2*[3] indicates an asymmetric pattern of hydrogen bonding to the cysteinyl sulfurs of the cluster. Moreover, NMR studies[51] of $[4Fe\text{-}4S]^{1+}$ *Av2* show a 3:1 pattern for the contact-shifted cysteinyl α-CH protons (but apparently not for the β-CH_2 protons).

To check whether one iron site might change coordination upon reduction of the cluster to the all-ferrous state, we performed a radiolytic reduction of the $[4Fe\text{-}4S]^+$ cluster at 77 K in a synchrotron beam.[52] This irradiation lead to a reduction of the cluster with nearly 60% yield and produced a state with EPR spectra identical to those of Ti(III)citrate-reduced *Av2*. This observation rules out the possibility that either ligand exchange or reorientation of cysteinyl ligands occurs between the 1+ and 0 states of the cluster. The radiolytic reduction experiment yielded another interesting result. The spectral shapes of the EPR resonances that connect various sublevels of the $S = 4$ multiplet (Figure 2) are determined to a large extent by distributions of the zero-field splitting parameters. These

(42) The following discussion, while instructive, is somewhat simplistic because it ignores geometric (cluster expansion) and covalency changes that occur upon changing oxidation states. For a discussion of these issues, the reader is referred to the work of Noodleman et al.[43]

(43) Noodleman, L.; Peng, C. Y.; Case, D. A.; Mouesca, J.-M. *Coord. Chem. Rev.* **1995**, *144*, 199−244.

(44) Gütlich, P.; Link, R.; Trautwein, A. In *Mossbauer Spectroscopy and Transition Metal Chemistry*; Springer-Verlag: Berlin, 1978; Chapter 6.

(45) Middleton, P.; Dickson, P. P. E.; Johnson, C. E.; Rush, J. D. *Eur. J. Biochem.* **1978**, *88*, 135−141. (b) Aizman, A.; Case, D. A. *J. Am. Chem. Soc.* **1982**, *104*, 3269−3279. (c) Papaefthymiou, V.; Girerd, J.-J.; Moura, I.; Moura, J. J. G.; Münck, E. *J. Am. Chem. Soc.* **1987**, *109*, 4703−4770. (d) Bominaar, E. L.; Hu, Zhengguo; Münck, E.; Girerd, J.-J.; Borsch, S. A. *J. Am. Chem. Soc.* **1995**, *117*, 6976−6989. (e) Bertini, I.; Ciurli, S.; Luchinat, C. *Structure and Bonding*; Springer-Verlag: Berlin, 1995; Vol. 83, pp 1−54.

(46) Lindahl, P. A.; Day, E. P.; Kent, T. A.; Orme-Johnson, W. H.; Münck, E. *J. Biol. Chem.* **1985**, *260*, 11160−11173.

(47) Middleton, P.; Dickson, D. P. E.; Johnson, C. E.; Rush, J. D. *Eur. J. Biochem.* **1980**, *104*, 289−296.

(48) The isomer shift of Fe^{3+}-rubredoxin from *Clostridium pasteurianum* has been reported to be 0.3 mm/s.[23] We have recently studied the same protein and obtained $\delta = 0.24 \pm 0.02$ mm/s.[49]

(49) Yoo, S. J.; Achim, C.; Meyer, J.; Münck, E., manuscript in preparation.

(50) Gamelin, D. R.; Bominaar, E. L.; Kirk, M. L.; Wieghardt, K.; Solomon, E. I. *J. Am. Chem. Soc.* **1996**, *118*, 8085−8097.

(51) Lanzilotta, W. N.; Holz, R. C.; Seefeldt, L. C. *Biochemistry* **1995**, *34*, 15646−15653.

(52) The X-ray structure of *Av2*[2,3] shows that each iron site of the cube is coordinated by one cysteinyl sulfur, i.e., all sites have tetrahedral sulfur coordination. The oxidation state of the cluster in *Av2* single crystals was not established by spectroscopic studies. Crystals were grown under anaerobic conditions in the presence of 2 mM dithionite;[3] however, it is well-known that *Av2* autooxidizes to the 2+ state in dithionite solutions.

distributions, in turn, reflect different conformations that the protein attains in frozen solution. Interestingly, the shapes of the EPR spectra were the same for the Ti(III)citrate-reduced and the radiolytically reduced samples, suggesting that the conformational distributions present in the frozen matrix (below 150 K) are the same in the 1+ and 0 states.

We have argued previously[27,53,54] on the basis of isomer shift data that the [8Fe-7S] P-clusters of the nitrogenase MoFe protein, in the dithionite reduced state P^N, are all-ferrous. The data obtained here support this interpretation. Interestingly, the P-cluster Mössbauer spectra exhibit two quadrupole doublets exhibiting a 3:1 intensity ratio. The major species, component D, has $\Delta E_Q \approx 0.8$ and 1.3 mm/s and $\delta \approx 0.63$ mm/s while the minor component, component Fe^{2+}, has $\Delta E_Q \approx 3$ mm/s and $\delta \approx 0.66$ mm/s.[27,53,54] Although there seem to be intriguing similarities between P^N and the all-ferrous *Av2* cluster, one should keep in mind that the P-clusters are double-cubanes and that it is possible that the 6:2 ratio reflects a case where one cube contains two Fe^{2+} and two D-sites while the other comprises four D-sites. In fact, Mouesca et al.[55] have assumed this case for their spin-coupling model for the state P^{ox}.

The $S = 4$ manifold of the all-ferrous cluster yields well-behaved EPR spectra that can be observed up to 140 K. These spectra consist of subspectra belonging to four different pairs of levels of the spin multiplet (Figure 2). Moreover, we have found EPR evidence for the population of an excited spin multiplet with (presumably) $S = 3$. We have been able to simulate all observed EPR features with a model that assumes that the rhombicity parameter E is distributed over a Gaussian. The only temperature-dependent quantity used in the simulation was the width of the spin packets which was allowed to increase from $\sigma_B = 0.25$ mT at 2 K to $\sigma_B = 0.68$ mT at 120 K; this increase can be attributed to lifetime broadening. Given that the observed EPR spectra contain resonances originating from different sublevels of the $S = 4$ multiplet, the simulations fit the data with remarkable accuracy. To our knowledge fits of a quality comparable to those presented here have not been published in the literature for any integer-spin system.

We have analyzed the exchange couplings among the six diiron pairs of all-ferrous *Av2* with the view of understanding the occurrence of an $S = 4$ ground state and of understanding the observation of the 3:1 pattern in the signs of the A-values. Little is known about the J-values of diferrous pairs in iron sulfur clusters, and we are not aware of published $J(Fe^{2+}Fe^{2+})$ values. There is a perception that $J(Fe^{3+}Fe^{3+}) > J(Fe^{3+}Fe^{2+}) > J(Fe^{2+}Fe^{2+})$, perhaps suggested by the observation that the cluster core expands upon reduction. However, the four short Fe−Fe distances (2.53 Å) indicated by the EXAFS analysis[41] suggest the possibility that some J-values may be larger than anticipated. In fact, our spin-coupling analysis suggests that the J-values of the all-ferrous cluster differ by at least a factor 3. The EPR evidence for the presence of a low-lying $S = 3$ multiplet does not shed much light on the magnitudes of J because small variations in any of the six unknown J-values will affect the energy separation between the ground $S = 4$ and the low-lying $S = 3$ multiplets. Moreover, the experimentally determined A_{iso}-values, in conjunction with analysis of the exchange couplings, show that the four sites cannot have the same intrinsic a_{iso}-values. We suspect that A_{iso} of Fe_A contains a substantial orbital contribution (if a smaller A_{iso}-value of Fe_A would reflect a larger degree of electron delocalization into the ligands, one would expect the isomeric shift of Fe_A to differ from those of sites 2−4, in contrast to the experimental observations). Finally, we wish to stress that the all-ferrous cluster has unusual electronic transitions, namely the 490 nm band whose MCD magnetization behavior is linked to the $S = 4$ multiplet.[56] A feature around 500 nm is unprecedented for $Fe^{2+}S_4$ sites. Thus, although the present study has provided substantial insight into the nature of the all-ferrous state, further spectroscopic and structural studies are required to probe this novel cluster state. In particular, its physiological relevance in dinitrogen reduction needs to be explored.

Acknowledgment. We thank Dr. Emile L. Bominaar, with whom we have enjoyed many fruitful discussions throughout the course of this work. We are also grateful for the efforts of Professor Timothy Elgren (Hamilton College) and Dr. Ernie Fontes (CHESS) for the sample irradiation at the Cornell High-Energy Synchrotron Source. This research was supported by National Science Foundation Grant MCB-9406224 (E.M.) and by National Institute of Health Grants GM-49970 (M.P.H.) and GM-45209 (B.K.B.).

JA9837405

(53) Huynh, V. H.; Henzl, M. T.; Christner, J. A.; Zimmermann, R.; Orme-Johnson, W. H.; Münck, E. *Biochim. Biophys. Acta* **1980**, *623*, 124−138.

(54) Surerus, K. K.; Hendrich, M. P.; Christie, P. D.; Rottgardt, D.; Orme-Johnson, W. H.; Münck, E. *J. Am. Chem. Soc*. **1992**, *114*, 8579−8590.

(55) Mouesca, J.-M.; Noodleman, L.; Case, D. A. *Inorg. Chem.* **1994**, *33*, 4819.

(56) Yoo, S. J.; Angove, H. C.; Burgess, B. K.; Münck, E.; Peterson, J. *J. Am. Chem. Soc.* **1998**, *120*, 9704−9705.